Bond Behaviour of Reinforced Fly Ash-Based Geopolymer Concrete Beams

Ee Hui Chang, Prabir Sarker, Natalie Lloyd, B Vijaya Rangan
Department of Civil Engineering
Curtin University of Technology
GPO Box U1987, Perth 6845
Western Australia

Synopsis: In view of sustainable development in the construction industry, investigation has been carried out on fly ash-based geopolymer concrete, which is an environmentally friendly material that uses geopolymer paste as binder instead of Portland cement. Previous studies on the engineering properties and structural behaviour of geopolymer concrete have shown promising potential of this material. This paper describes the bond behaviour between geopolymer concrete and reinforcing bars in tensile splices in beams. Twelve full-scale beam specimens with lap-spliced reinforcing bars were cast and tested in the laboratory to study the bond performance of geopolymer concrete. The effects of concrete compressive strength, bar diameter and splice length of the bars on bond strength of lap splices in geopolymer concrete were evaluated. Test results, including general behaviour of beams, failure modes and cracking patterns were gathered and analysed. Current analytical models and codes provision to predict bond strength for Ordinary Portland Cement (OPC) concrete were used to analyse the bond strength of test specimens. Good correlation between test and analytical results were found. This study also demonstrates the excellent potential of geopolymer concrete for use as a construction material.

Keywords: beams, bond behaviour, splice strength, geopolymer concrete

1. Introduction

Geopolymers are emerging materials which, since being proposed by Davidovits in 1979, have been used in applications ranging from waste management to the building industry. Their difference in chemical process and matrix formation means geopolymers have technical performance advantages over conventional cement binders, such as early compressive strength gain, higher acid and fire resistance, low alkali-aggregate expansion and sulphate and corrosion resistance (1,2,3,4,5). In addition, with correct mix design and formation development, fly ash-based geopolymer concrete can exhibit superior chemical and mechanical properties to those of Portland cement concrete (6). All of these benefits make geopolymers promising construction materials.

Studies on structural applications of fly ash-based geopolymer concrete are important, not only because of the difference in terms of chemical reaction and matrix formation compared to Portland cement concrete, but also because of the need to examine the suitability of current code provisions and theories for Portland cement concrete to be used for geopolymer concrete. The lap splice of reinforcing bars is one of the practical aspects of bond between concrete and reinforcing bars. Given their inevitable use in most reinforced concrete structures, accurate prediction of splice length is important as the performance of reinforced concrete structures depends on adequate bond between concrete and reinforcing steel. The present research is therefore dedicated to the study of the bond performance of lap splices in geopolymer concrete beams.

2. Fly Ash-Based Geopolymer Concrete

Geopolymer concrete is manufactured by using by-products such as fly ash that are rich in silicon and aluminium. The chemical composition of the fly ash is determined using an X-Ray Fluorescence (XRF) analysis. The silicon and aluminium oxides in low-calcium fly ash constitute about 80% by mass, with the atomic ratio of Si-to-Al of about 2, which is suitable for making concrete (7). The alkaline liquid, which is a combination of sodium silicate solution and sodium hydroxide solution, react with the silicon and aluminium in the fly ash to form the paste which binds the loose coarse and fine aggregates to produce the geopolymer concrete. The coarse and fine aggregates currently used by the concrete industry are found to be suitable for producing geopolymer concrete. As in the case of OPC concrete, the coarse and fine aggregates occupy about 75% to 80% of the mass of geopolymer concrete. Also, the manufacture of geopolymer concrete is carried out using the usual concrete technology methods.

In order to improve the workability, a high range water reducer super plasticizer and any extra water may be added to the mixture.

The engineering properties of geopolymer concrete, including compressive strength, indirect tensile strength, modulus of elasticity and Poisson's ratio have been reported by Hardjito and Rangan (8) and Sofi et al. (9). These properties compare favourably to those predicted by the relevant Australian Standards for Portland cement concrete. The studies of long-term properties by Wallah and Rangan (10) show that fly ash-based geopolymer concrete undergoes very little shrinkage.Test data also show that geopolymer concrete has excellent resistance to sulfate attack. On the studies of structural application of heat-cured fly ash-based geopolymer concrete, reinforced columns and beams were manufactured and tested. Test results show that the behaviour, failure mode and load carrying capacity of column members were similar to that of OPC concrete, and good correlations of results were obtained by using current calculation methods for OPC concrete (11). The behaviour and failure mode of beams tested in flexure were also observed to be similar to that of OPC concrete. The results of flexure capacity and deflection of beams agree well with the current design provisions used for OPC concrete members (11).

The bond performance of reinforcing bars in geopolymer mortars and concrete has been studied by Sofi et al. (12). A total of 27 beam-end specimens and 58 cubic direct pullout-type specimens were manufactured and tested. A splitting type of failure was observed for all beam-end specimens, and the failures were irrespective of the size of reinforcing bar. They find that all beam specimens failed by splitting of concrete surrounding the bar, and that the normalised bond strength increased with a reduction in rebar size. Conservative results were obtained when the test results were compared with predictions from code provisions such as AS3600, ACI 318 and Eurocode 2.The bond strength of geopolymer concrete was also investigated by Sarker et al. (13). A total of 24 geopolymer concrete and 6 Portland cement beam-end specimens were tested to study the bond behaviour of geopolymer concrete. From the analysis of results, it was found that both geopolymer concrete and Portland cement concrete specimens show similar patterns of bond stress-slip graphs. The design expressions proposed by Orangun et al. (14), Esfahani and Rangan (15) and ACI-408R (16) resulted in conservative predictions of bond strength for both geopolymer concrete and Portland cement concrete.

3. Experimental Program

3.1 Test Specimens

The test program consisted of twelve lap-spliced beam specimens with a cross section of 200 mm x 300 mm. All beam specimens were 2500 mm long. The size of test specimen was selected to suit the capacity of the testing machine in the laboratory. In order to obtain a bond splitting mode of failure, all splice lengths were chosen to develop steel stress less than yield at failure. No transverse reinforcement was provided in the splice region. The beams were divided into two series to investigate the test parameters of bond strength: concrete cover, bar diameter, splice length and concrete compressive strength. The complete details of the beams are given in Table 1. The geometry and details of beams are shown in Figure 1.

Table 1: Beam Details

Series	Beam Mark	Compressive Strength f'_c (MPa)	Bar Diameter d_b (mm)	Splice Length L_s (mm)	Bottom Cover c_b (mm)	Side Cover c_{so} (mm)	Half of Spacing Between Spliced Bars c_{si} (mm)	C/d_b Ratio	L_s/d_b Ratio
D	N-D-1.0	37	24	355	30	32	20	1.1	14.8
	N-D-1.5	37	20	303	30	32	28	1.5	15.2
	N-D-2.2	30	16	240	40	38	29	2.2	15.0
	H-D-1.0	55	24	356	25	28	25	1.0	14.8
	H-D-1.5	55	20	301	30	38	24	1.5	15.1
	H-D-2.2	48	16	243	40	39	28	2.2	15.2
L	N-L-12.5	30	24	300	31	27	25	1.1	12.5
	N-L-18.8	29	24	452	25	27	23	1.0	18.8
	N-L-30.0	29	24	723	25	28	25	1.0	30.1
	H-L-12.5	48	24	300	27	27	24	1.1	12.5
	H-L-18.8	51	24	455	25	30	22	1.0	19.0
	H-L-30.0	51	24	722	25	30	24	1.0	30.1

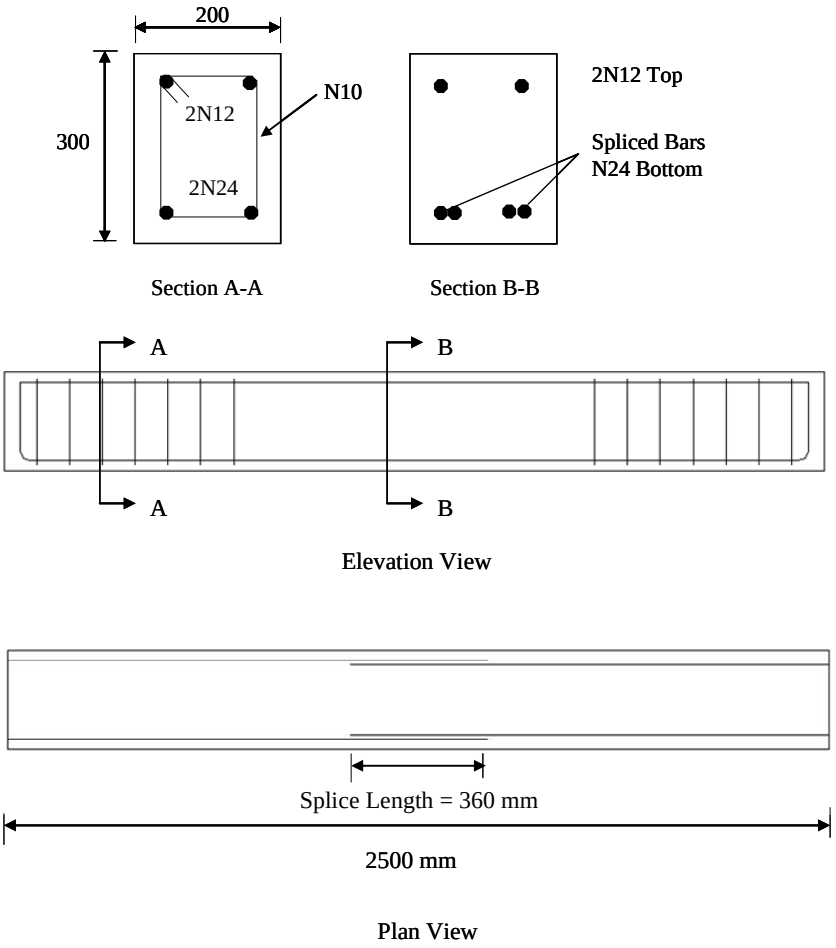

Figure 1: Geometry and Reinforcement Arrangement for Beams N-D-1.0 and H-D-1.0

3.2 Materials

3.2.1 Geopolymer Concrete

In this study, low-calcium (ASTM C 618, Class F) fly ash obtained from Collie Power Station in Western Australia was used as base material. The chemical composition of the fly ash as determined by the X-Ray Fluorescence (XRF) analysis is given in Table 2. Locally available aggregates comprising 10mm and 7mm crushed granite-type coarse aggregates and fine concrete sand were used. The aggregates were prepared to be in a saturated-surface-dry (SSD) condition. The fineness modulus of the combined aggregates was determined as 4.5. The alkaline liquid used was a combination of sodium hydroxide and sodium silicate solutions. The sodium hydroxide solution was made by dissolving the NAOH solids (pellet form) of commercial grade with 97% purity in distilled water and was prepared at least 24 hours prior to use. In this study, a concentration of 14 Molars was used throughout. The sodium silicate solution used was Grade A53 with a chemical composition of Na_2O=14.7%, SiO_2=29.4%, and water=55.9% by mass. To improve the workability of fresh geopolymer concrete, a commercially available naphthalene sulphonated super plasticizer was used (11).

Table 2: Chemical composition of fly ash (mass %)

SiO_2	Al_2O_3	Fe_2O_3	CaO	Na_2O	K_2O	TiO_2	MgO	P_2O_5	SO_3	H_2O	LOI*
50.8	26.9	13.5	2.05	0.33	0.57	1.57	1.33	1.46	0.31	-	1.42

** Loss on ignition*

3.2.2 Steel Reinforcement

All the reinforcement used in this study was standard deformed bar designed to give a minimum yield strength of 500MPa. In order to obtain the actual yield strength and ultimate strength of the reinforcement, three sample bars of each size, from the same batch of steel production, were tested in the laboratory. The summary of the test results is given in Table 3, and shows the mean value and range. These results will be used in the calculation and analysis of the beams.

Table 3: Steel Reinforcement Properties

Nominal Diameter (mm)	Nominal Area (mm^2)	Yield Strength (MPa)	Ultimate Strength (MPa)
10	78.5	554 ± 3	637 ± 2
16	200	539 ± 5	638 ± 5
20	310	564 ± 3	653 ± 5
24	450	563 ± 3	655 ± 4

3.3 Mixture Proportions for Geopolymer Concrete

Several trial mixes were prepared according to mixture proportions developed by Sumajouw and Rangan (11) to obtain mean compressive strengths of 35 MPa and 55 MPa. From these trial mixes, the mixture proportion with the designation GP1 and GP2 were selected. For GP2, the compressive strength was obtained with steam curing of 24 hours at 60ºC and three rest days prior to curing. The details of the mixture proportion for GP1 and GP2 are given in Table 4. It can be seen that the only difference between the two mixtures is the mass of extra water added.

Table 4: Mixture proportions of geopolymer concrete

Material	GP1	GP2
	Mass (kg/m^3)	Mass (kg/m^3)
Aggregate 10mm	551	556
Aggregate 7mm	643	650
Sand	643	650
Fly Ash	406	410
Sodium Hydroxide Solution (14M)	41	41
Sodium Silicate Solution	103	103
Superplasticiser	6.1	6.1
Extra added water	25.6	16.5
Rest Period (days)	None	3 days

3.4 Manufacture and Curing of Geopolymer Concrete

The manufacture and curing process of geopolymer concrete were based on earlier research (8). Due to the limited capacity of pan mixer, five batches of geopolymer concrete were prepared to cast two beam specimens for each pour. The fly ash, coarse aggregates (10mm and 7mm) and sand were first mixed dry in the laboratory pan mixer (70-litre capacity) for about three minutes. Next the alkaline liquid, together with the super plasticiser and the extra water, were mixed together and added into the dry mixture. The mixing continued for another four minutes. After mixing, a slump test was used to measure the workability of every batch of geopolymer concrete. Once the mixing of the geopolymer concrete was complete, it was immediately cast into the moulds for beam specimens and cylinder test specimens. The fresh geopolymer concrete was placed into the mould in layers. A stick internal vibrator was used to compact the fresh geopolymer concrete in the mould. For each batch of concrete, at least three 100mm x 200mm diameter cylinders were cast. A total of six 150mm x 300mm diameter cylinders were also cast for splitting tensile tests, to obtain the tensile strength of geopolymer concrete. All the cylinders were compacted and cured in the same manner as the beams, and were tested at the same time as the beam tests. After curing, all specimens were removed from the chamber, de-moulded, and left in ambient conditions in the laboratory until the time of testing.

3.5 Beam Test Set-Up and Testing Procedure

All beams were simply supported over a span of 2300mm. The beams were tested and loaded to failure by a 2500 kN-capacity Universal test machine in the laboratory. Three Linear Variable Differential Transducers (LVDTs) were used to measure the vertical deflections of test beams. A 50mm plunger travel LVDT was located at the mid-span, while two 50mm plunger travel LVDTs were placed under the applied concentrated loads. Prior to testing, all beams were whitewashed to facilitate the marking of cracks. A preload of 20kN was applied to ensure that the test set-up and instrumentation worked properly. The beam was then unloaded and datum readings were taken.

The test was conducted by moving the test machine platen at a ram rate of 0.3mm per minute, which provided sufficient time of crack observation and marking during beam tests. The locations of cracks were marked during the process of testing, until failure. The duration of each test was 20 to 30 minutes.

4. Test Results and Observations

4.1 Failure Mode and Crack Patterns

Twelve beams were tested under monotonically increasingly load until failure. The behaviour of all test beams was similar. All beams failed by splitting of the concrete at the tension face within the splice region. In general, the first flexural cracks for all beams formed initially on the tension face in the constant moment region. As the load increased, cracks formed along the entire length of the constant moment zone including the splice region. Failure occurred just after the longitudinal splitting cracks formed in the bottom cover on the tension side of beam at the splice region, and in the side cover at the levels of the splice. It was observed that when compared to normal strength geopolymer concrete beams, the high strength geopolymer concrete beams failed in a more brittle manner. Generally, this is expected and is similar to what is observed in Portland cement concrete specimens reported in the literature (15, 17, 18, 19). Typical crack patterns at the splice region at both the side face and bottom face of Beam N-D-1.0 are shown in Figure 2.

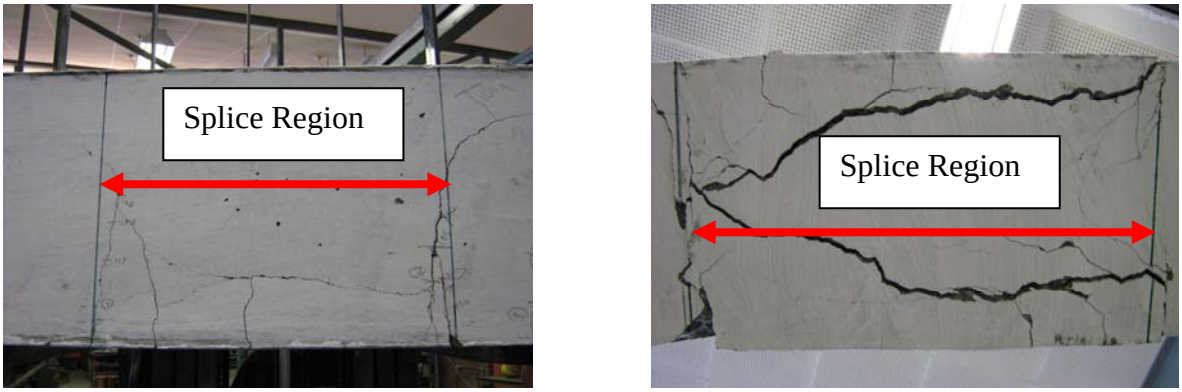

Figure 2: Crack Pattern of Beam N-D-1.0 over the Splice Region After Failure (Side Face and Bottom Face)

4.2 Summary of Test Results

The average bond stress was calculated using Equation 1 obtained by evaluating the total force developed in the bar, $A_b f_s$ divided by the bar surface area over the splice length given by

$$u = \frac{A_b f_s}{\pi d_b L_s} = \frac{f_s d_b}{4 L_s} \quad (1)$$

where
u = Average bond stress (MPa); A_b = Area of one bar ; d_b = Diameter of bar ; L_s = Splice length and f_s = Stress in the tensile steel.

All the beams were designed as under-reinforced beams and all the splice lengths were designed to develop steel stress less than yield stress at failure. The steel stress, f_s, was determined based on elastic cracked section analysis by using the transformed section analysis as given in Equation 2.

$$f_s = \frac{M_{\max}}{A_{st}\, jd} \tag{2}$$

where
M_{max} = Maximum bending moment when bond failure occurred; A_{st} = Area of tensile steel ; jd = Lever arm; the lever arm coefficient was calculated by performing a conventional elastic analysis of a fully cracked transformed section.

From the test results of the sample bars used for the test specimens, the yield stresses of bars of 24mm, 20mm, and 16mm were 563 MPa, 564 MPa and 539 MPa respectively. It can be seen that the calculated steel stress values from Table 5 were less than the yield stresses of the steel tested. Therefore, the method based on elastic analysis to determine the steel stress was considered to be acceptable to calculate the average bond stress of the test specimens.

Table 5: Summary of Test Results

Series	Beam Mark	f'_c (MPa)	C/d_b Ratio	L_s/d_b Ratio	Failure Load P_{max} (kN)	Maximum Bending Moment M_{max}^* (kNm)	Steel Stress f_s (MPa)	Average Bond Stress u (MPa)
D	N-D-1.0	37	1.1	14.8	165.2	58.7	292.5	4.94
	N-D-1.5	37	1.5	15.2	145.5	51.8	365.6	6.03
	N-D-2.2	30	2.2	15.0	111.0	39.7	440.5	7.34
	H-D-1.0	55	1.0	14.8	194.8	69.1	334.2	5.63
	H-D-1.5	55	1.5	15.1	172.6	61.3	429.5	7.13
	H-D-2.2	48	2.2	15.2	135.7	48.4	532.6	8.77
L	N-L-12.5	30	1.1	12.5	135.7	48.4	242.5	4.85
	N-L-18.8	29	1.0	18.8	194.8	69.1	339.2	4.50
	N-L-30.0	29	1.0	30.1	249.1	88.1	432.5	3.59
	H-L-12.5	48	1.1	12.5	167.7	59.6	292.1	5.84
	H-L-18.8	51	1.0	19.0	251.6	88.9	432.5	5.70
	H-L-30.0	51	1.0	30.1	323.1	114.0	554.2	4.61

*Note: * including the moment due to self-weight of the beam and loading system*

4.3 Effect of Parameters on Bond Strength

4.3.1 Effect of C/d_b

Three C /d_b ratios, 1.0, 1.5 and 2.2 (for bar diameters of 24 mm, 20 mm and 16 mm respectively), were used in six geopolymer concrete beams. For each C/d_b ratio, two companion beams with different concrete strengths were tested; these were Beams N-D-1.0 and H-D-1.0; N-D-1.5 and H-D-1.5; N-D-2.2 and H-D-2.2.The effect of C/d_b ratio on bond strength for each pair of geopolymer concrete beams is presented in Figure 3. It can be seen that the bond stress increases as C/d_b increases (or bar size decreases) for both normal strength (represented by N-series) and high strength (represented by H-series) geopolymer concrete. This trend is similar to what is observed for Portland cement concrete beams and reported in the literature (20). Sofi et al. (12) observe that the normalised bond strength increases with a reduction in bar size for low calcium fly ash geopolymer mortar and concrete beam-end specimens. The trend of test results observed in their study is similar to what is observed in this study.

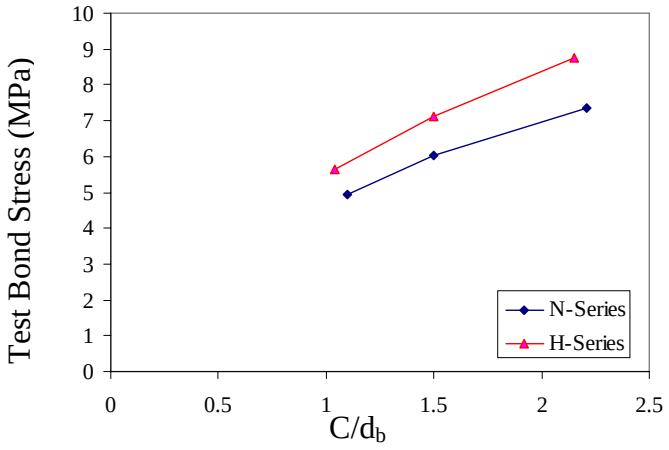

Figure 3: Effect of C/d_b on Bond Stress

4.3.2 Effect of L_s/d_b

Three L_s/d_b ratios, 12.5, 18.8 and 30.0, were used in six geopolymer concrete beams. For each L_s/d_b ratio, two companion beams with different concrete strengths were tested; these were Beams N-L-12.5 and H-L-12.5; N-L-18.8 and H-L-18.8; N-L-30.0 and H-L-30.0. The effect of L_s/d_b on bond strength for each pair of geopolymer concrete beams is presented in Figure 4. As L_s/d_b increases, the bond stress decreases for both normal strength (represented by N-series) and high strength (represented by H-series) geopolymer concrete. This observation is found to be similar to the reported literature from Azizinamini et al. (21) for Portland cement concrete beams.

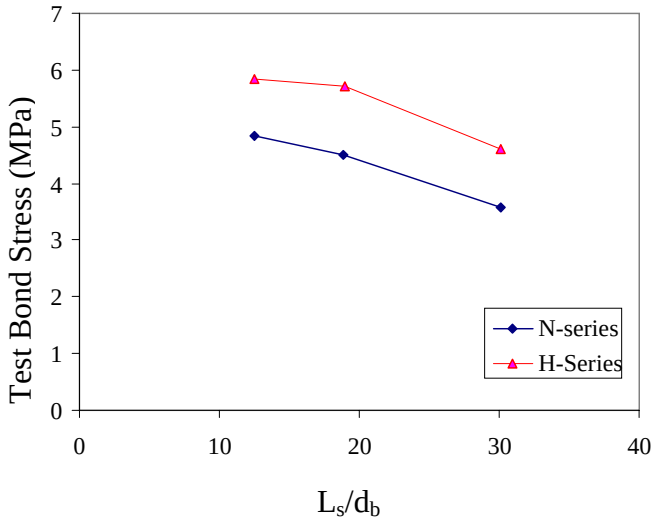

Figure 4: Effect of L_s/d_b on Bond Stress

4.3.3 Effect of Concrete Compressive Strength

Two types of concrete compressive strength, represented by normal strength and high strength given by the mix designs GP1 and GP2 respectively, were used in this study. For D-Series with C/d_b ratios as the parameter, it can be seen from Figure 5 that bond stress increased with the increase in compressive strength for the same C/d_b ratio in all cases. This trend is similar to what was observed by Sarker et al. (13) on the effect of compressive strength on bond strength for geopolymer concrete beam-end specimens with C/d_b ratios ranging from 1.8 to 3.2. For L-Series with L_s/d_b ratios as parameter, it can be seen from Figure 6 that bond stress increases with the increase in compressive strength for the same L_s/d_b ratio in all cases.

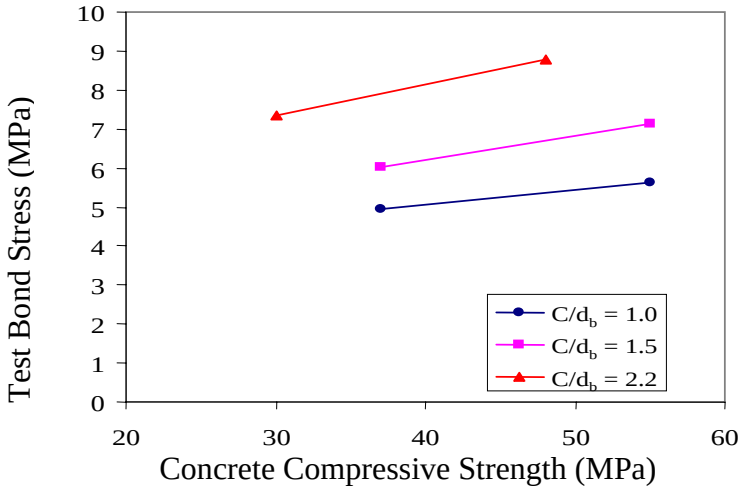

Figure 5: Effect of Concrete Compressive Strength on Bond Stress for D-Series

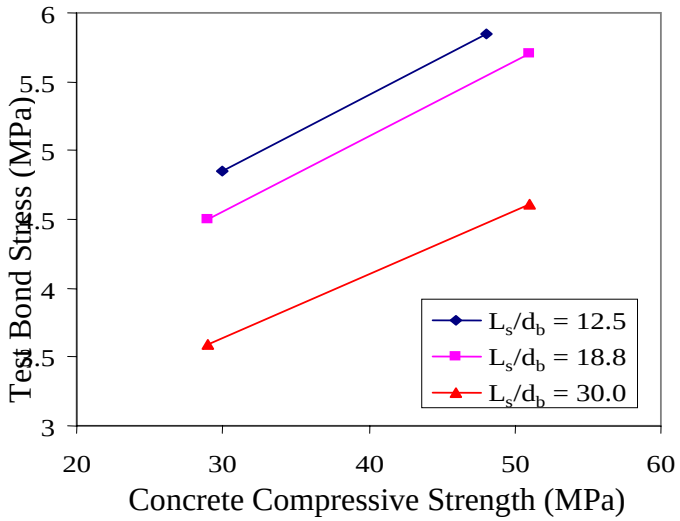

Figure 6: Effect of Concrete Compressive Strength on Bond Stress for L-Series

5. Correlation of Test and Calculated Bond Strength of Geopolymer Concrete

The bond strength of lap splices of geopolymer concrete beams was predicted using the current analytical models and code provisions for Portland cement concrete. The analytical models include Orangun et al. (14), Zuo and Darwin (19), ACI408R-03 (16), Esfahani and Rangan (15) and Canbay & Frosch (20). Code provisions such as AS3600-01 (22), draft AS3600 (23) and ACI318-08 (24) are used. The summary of the results correlation using the above mentioned is given in Table 6. From Table 6, it can be seen that the analytical model proposed by Canbay & Frosch (20) predicts the bond strength of tensile splices of geopolymer concrete beams most accurately, with an average test-to-prediction ratio of 1.17 and coefficient of variation of 11.97%. Other models yielded similar predictions for the bond strength of all beams, with an average test-to- prediction ratio of 1.25 to 1.30. The code provisions are found to be conservative in predicting the bond strength of geopolymer concrete beams. From Table 6, it can be seen that the average test-to-prediction ratio by AS3600-01(22) is 2.03 with a coefficient of variation of 10.84%. Both draft AS3600 (23) and ACI 318-08 (24) predict similar average test-to-prediction ratios, of 1.74 and 1.70 respectively, with a smaller coefficient of variation of 8.82% given by ACI 318-08 (24).

Table 6: Summary of Results for Correlation of Test and Calculated Bond Strength of Geopolymer Concrete

	Test/Predicted Ratio								
Beam Mark	Orangun	Zuo & Darwin	ACI408R-03	Esfahani & Rangan	Canbay & Frosch	Canbay & Frosch (using actual f'_{ct} from test)	AS3600-01	AS3600-05 Draft	ACI 318-08
N-D-1.0	1.29	1.13	1.11	1.16	1.17	0.98	2.30	1.67	1.66
N-D-1.5	1.28	1.27	1.25	1.20	1.21	1.01	1.97	1.86	1.77
N-D-2.2	1.50	1.43	1.42	1.06	1.38	1.28	2.19	2.35	1.60
H-D-1.0	1.11	1.16	1.14	1.33	1.08	0.98	1.86	1.51	1.76
H-D-1.5	1.33	1.37	1.36	1.26	1.16	1.06	2.14	1.87	1.72
H-D-2.2	1.45	1.55	1.53	1.12	1.31	1.01	2.12	2.25	1.51
N-L-12.5	1.19	1.06	1.04	1.21	1.27	1.17	2.17	1.76	1.77
N-L-18.8	1.40	1.24	1.22	1.42	1.22	1.12	2.16	1.68	1.94
N-L-30.0	1.25	1.20	1.19	1.36	0.94	0.86	1.63	1.32	1.54
H-L-12.5	1.16	1.13	1.12	1.28	1.22	0.94	2.12	1.69	1.85
H-L-18.8	1.36	1.35	1.34	1.51	1.14	0.87	2.13	1.62	1.85
H-L-30.0	1.24	1.31	1.30	1.41	0.91	0.69	1.62	1.29	1.49
Average	1.30	1.27	1.25	1.28	1.17	1.00	2.03	1.74	1.70
S.D.	0.12	0.14	0.14	0.13	0.14	0.15	0.22	0.32	0.15
COV (%)	9.23	11.02	11.20	10.16	11.97	15.21	10.84	18.39	8.82

The analytical expression proposed by Canbay and Frosch (20) is based on a physical model of tension cracking of concrete in the lap-spliced region. In this model, the tensile strength of concrete surrounding the bar is a major parameter that affects the development of the reinforcement for a splitting failure. The bond strength of lap splices of all beams was re-calculated based on the measured tensile strength of geopolymer concrete using the Canbay and Frosch model. It was found that when using the measured tensile strength of geopolymer concrete from the splitting tensile cylinders tested, an improved correlation of test and calculated bond strength for geopolymer concrete beams was obtained. From Table 6, it can be seen that the average test-to-prediction ratio is 1.0 with coefficient of variation of 15.21%.The studies conducted by Hardjito and Rangan (8), Gourley and Johnson (25) and Sofi et al. (9) show that the tensile strength of geopolymer concrete is larger than that of Portland cement concrete, and that there is a close relationship between the splitting tensile strength and the bond strength of geopolymer concrete. This indicates that higher tensile strength of geopolymer concrete contributes to the higher bond strength of geopolymer concrete when compared to Portland cement concrete.

6. Conclusions

A total of twelve lap-spliced geopolymer concrete beams were manufactured and tested to study the bond behaviour. No transverse reinforcement was provided in the splice region. The beams were 200 mm wide, 300 mm deep and 2500 mm long. The effect of concrete cover, bar diameter, splice length and concrete compressive strength on bond strength were studied. The failure mode and crack patterns observed for reinforced geopolymer concrete beams were similar to those reported in the literature for reinforced Portland cement beams. The bond strength of geopolymer concrete was observed to be closely related to the tensile strength of geopolymer concrete. Good correlation of test bond strength with predictions from the analytical model proposed by Canbay and Frosch (20) were obtained when using the actual tensile strength of geopolymer concrete. The average ratio of test bond strength to predicted bond strength was 1.0 with a coefficient of variation of 15.21%. It was found that the design provision and analytical models used for predicting bond strength of lap-splices in reinforced Portland cement concrete are applicable to reinforced geopolymer concrete beams.

7. Acknowledgement

The first author is a recipient of a Curtin University Postgraduate Scholarship (CUPS).

8. References

1. Lee, W.K.W. and van Deventer, J.S.J. (2002). "The Effect of Ionic Contaminants on the Early-Age Properties of Alkali-Activated Fly Ash-Based Cements", *Cement and Concrete Research*, 32(4), 577–584.
2. Davidovits, J. (1991). "Properties of Geopolymer Cements", *Journal of Thermal Analysis*, 37, 1633–1656.
3. García-Lodeiro, I., Palomo, A. and Fernández-Jiménez, A. (2007). "Alkali-aggregate Reaction in Activated Fly Ash Systems", *Cement and Concrete Research*, 37, 175–183.
4. Bakharev, T. (2005a). "Resistance of Geopolymers Materials to Acid Attack", *Cement and* Concrete Research, 35 (6), 658–670.
5. Bakharev, T. (2005b). "Durability of Geopolymer Materials in Sodium and Magnesium Sulfate Solutions", *Cement and Concrete Research*, 35 (6), 1233–1246.
6. Duxson, P., Fernández-Jiménez, A., Provis, J.L., Lukey, G.C., Palomo, A. and van Deventer, J.S.J. (2007a). "Geopolymer Technology: The Current State of the Art", *Journal of Material Science*, 42, 2917–2933.
7. Davidovits, J. (1999). "Chemistry of Geopolymeric Systems, Terminology", *Proceedings of the Geopolymer 2005 World Congress*, Saint-Quentin, France.
8. Hardjito, D. and Rangan, B.V. (2005). "Development and Properties of Low-Calcium Fly Ash-Based Geopolymer Concrete", Research Report GC1, Faculty of Engineering, Curtin University of Technology, available at espace@curtin or www.geopolymer.org
9. Sofi, M., van Deventer, J.S.J., Mendis, P. and Lukey, G.C. (2007a). "Engineering Properties of Inorganic Polymer Concretes (IPCs)", *Cement and Concrete Research*, 37 (2), 251–257.
10. Wallah, S.E. and Rangan, B.V. (2006). "Low-calcium Fly Ash-based Geopolymer Concrete: Long Term Properties", Research Report GC2, Faculty of Engineering, Curtin University of Technology, Western Australia, available at espace@curtin or www.geopolymer.org
11. Sumajouw, M.D.J. and Rangan, B.V. (2006). "Low-Calcium Fly Ash-Based Geopolymer Concrete: Reinforced Beams and Columns", Research Report GC3, Faculty of Engineering, Curtin University of Technology, Western Australia, available at espace@curtin or www.geopolymer.org
12. Sofi, M., van Deventer, J.S.J., Mendis, P. and Lukey, G.C. (2007b). "Bond Performance of Reinforcing Bars in Inorganic Polymer Concrete (IPC)", *Journal of Materials Science*, 42 (9), 3007–3016.
13. Sarker, P.K., Grigg, A. and Chang, E.H. (2007). "Bond Strength of Fly Ash-Based Geopolymer Concrete With Reinforcing Bars", *Proceedings of Recent Developments in Structural Engineering*, Mechanics and Computation, CD ROM, Ed. A. Zingoni, Millpress, Netherlands.
14. Orangun, C. O., Jirsa, J. O. and Breen, J. E. (1977). "A Reevaluation of Test Data on Development Length and Splices", *ACI Journal*, 74 (3), 114–122.
15. Esfahani, M.R. and Rangan, B.V. (1998). "Bond between Normal Strength and High Strength Concrete (HSC) and Reinforcing Bars in Splices in Beams", *ACI Structural Journal*, 95 (3), 272–280.
16. ACI Committee 408 (2003). *408R–03: Bond Development of Straight Reinforcing Bars in Tension*, American Concrete Institute, Farmington Hills, MI.
17. Hamad, B.S. and Mike, J.A. (2003). "Experimental Investigation of Bond Strength of Hot-Dip Galvanized Reinforcement in Normal- and High-Strength Concrete", *ACI Structural Journal*, July–August, 465–470.
18. Hamad, B.S. and Itani, M.S. (1998). "Bond Strength of Reinforcement in High-Performance Concrete: The Role of Silica Fume, Casting Position, and Superplasticizer Dosage", *ACI Structural Journal*, September–October, 499–511.
19. Zuo, J. and Darwin, D., (2000). "Splice Strength of Conventional and High Relative Rib Area Bars in Normal and High Strength Concrete", *ACI Structural Journal*, 97 (4), July–Aug, 630–641.
20. Canbay, E. and Frosch, R.J. (2005). "Bond Strength of Lap-Spliced Bars", *ACI Structural Journal*, 102 (4), July–Aug, 605–614.
21. Azizinamini, A., Stark, M., Roller, J.J. and Ghosh, S.K. (1993). "Bond Performance of Reinforcing Bars Embedded in High-Strength Concrete", *ACI Structural Journal*, 90 (5), Sept–Oct., 554–561.
22. Standards Australia (2001). "Concrete Structures, AS3600–2001."
23. Committee BD-002 Standards Australia (2005). *Concrete Structures: Draft Australian Standard AS3600-2005*, Standards Australia.
24. ACI Committee 318 (2008). *Building Code Requirements for Structural Concrete*, *ACI 318–08*, American Concrete Institute, Farmington Hills, MI.
25. Gourley, J.T. and Johnson, G.B. (2005). "Developments in Geopolymer Precast Concrete", *Proceedings of the Geopolymer 2005 World Congress*, Saint-Quentin, France, 139–143.